In situ electron beam irradiated rapid crystallization of bismuth nanoparticles in bismuth glass dielectrics at room temperature

Shiv Prakash Singh . Basudeb Karmakar

Abstract In this work, in situ control growth of bismuth nanoparticles (Bi^0 NPs) was demonstrated in bismuth glass dielectrics under an electron beam (EB) irradiation at room temperature. The effects of EB irradiation were investigated in situ using transmission electron microscopy (TEM), selected-area electron diffraction (SAED) and high-resolution transmission electron microscopy (HRTEM). The EB irradiation for 2 to 8 min enhanced the construction of bismuth nanoparticles with a rhombohedral structure and diameter of 4-11 nm. The average particle size was found to increase with the irradiation time. Bismuth metal has a melting point of 271^0C and this low melting temperature makes easy the progress of energy induced structural changes during in situ TEM observations. This is a very useful technique in nano-patterning for integrated optics and other applications.

Keywords Bismuth nanoparticles . Transmission electron microscopy . Glass . Nanopatterning

---

Shiv Prakash Singh . Basudeb Karmakar*
Glass Science and Technology Section, Glass Division
Central Glass and Ceramic Research Institute (CSIR, India)
196 Raja S.C. Mullick Road, Kolkata 700 032, West Bengal, India
e-mail: basudebk@cgcri.res.in

Introduction

Recently, new and useful optical and electronic effects associated with metal, semiconductor and oxide nanocrystals have been discovered (Wang et al. 2005; Grzelczak et al. 2008). The inherent properties of a metallic nanostructure can be monitored by controlling its shape, size, composition, and crystallinity. The shape-control of these nanocrystals is very effective in tailoring the properties and functions of the metallic nanostructures. Whereas, the particle size of the crystalline materials approaches to the nanometer range exhibits a variety of interesting optical, electronic, and magnetic features (Wang et al. 2010; Jana et al. 2001; Wang et al. 2008; Balan et al. 2004).

Electron beam (EB) irradiation is a powerful technique that has recently attracted interest of various researchers as an effective tool for in-situ generation of various nanocrystals in different hosts (Kim et al. 2007; Sepulveda-Guzman et al. 2007; Kim et al. 2005). In the particular case of metallic nanoparticles, electron beam irradiation offers the advantage such as much higher local concentration of nanocrystal precipitates can be achieved than those produced in other methods. The bulk glass exhibited enhanced third-order optical nonlinearity effects by conventional approaches; on the other hand, electron beam irradiation produces significant radiation effects in the host glass material. The glass samples were used as suitable materials as the glassy state is considered to have a higher homogeneity than that of other sintered materials. Thus the electron beam irradiation effect can lead to extraordinary microstructures or large size dispersions of embedded nanocrystal in the host glass materials. Such extraordinary nanostructure

formed as a result of electron beam irradiation may be exploited and find use in future generations of optical devices.

Over the past few years, bismuth nanostructures have been extensively studied because of their magnetoresistance and excellent thermoelectric properties (Gao et al. 2003; Derrouiche et al. 2010; Carotenuto et al. 2009). The ability to synthesize well-defined and synthetically tunable nanoparticles could bring in new opportunities for fundamental studies as well as provide new viewpoint for various technological applications. Bismuth, a semimetal with a rhombohedral structure, possesses many useful properties such as it has a small energy overlap between the conduction and valence bands, high carrier motilities, and highly anisotropic Fermi surface that make it attractive for different applications (Wang et al. 2005; Wang et al. 2008; Grass et al. 2006). Small effective mass makes bismuth nanoparticles an interesting scheme for studying quantum confinement effects (Gao et al. 2003; Gekhtman et al. 1999). Recent work also has suggested that Bi materials of reduced dimensions may exhibit enhanced thermoelectric properties at room temperature (Zhang et al. 1999).

Various researchers have carried out different experiments on the change of morphology of bismuth nanoparticles under the electron beam irradiation in TEM. Kim et al. 2007 have studied controlled growth of bismuth nanoparticles from bismuth trichloride by electron beam irradiation in TEM with respect to time. Sepulveda-Guzman et al. 2007 have synthesized bismuth nanoparticles from sodium bismuthate and exposed to an electron beam at room temperature in a transmission electron microscope (TEM). The electron beam irradiation exhibited rhombohedral structure of bismuth nanoparticles with diameter of 6 nm. The one-pot fabrication of thiol-stabilized monodisperse gold

nanoparticles was reported by Kim et al. 2005 through the electron beam irradiation with highly ordered supramolecular structures.

With best of our knowledge, there is no any report on transmission electron microscope (TEM) based study on the formation of bismuth nanocrystals under electron beam irradiation in the bismuth glass dielectrics. The bismuth glass dielectric is it self a very fascinating material from the point of view of various technological applications. Therefore, in this work, we demonstrated how the effect of electron beam irradiation is used to good advantage in the formation of bismuth nanocrystals in bismuth glass dielectrics.

Experimental

High purity bismuth trioxide, Bi_2O_3 (Loba Chemie), boric acid, H_3BO_3 (Loba Chemie), zinc oxide, ZnO (Loba Chemie), potassium carbonate, K_2CO_3 (Loba Chemie), silicon dioxide, SiO_2 (Bremthaler/Quarzitwerk) and potassium peroxodisulphate, $K_2S_2O_8$ (Merck) were used as raw materials to prepare glasses. 25 g glass dielectric of composition (wt %) $19B_2O_3$-$23ZnO$-$45Bi_2O_3$-$9SiO_2$-$(4-x)K_2O$- $xK_2S_2O_8$, where x = 0 and 0.5 was melted in a 50 ml high purity silica crucible at 1100^{o}C in air for 30 min in a raising hearth electrical furnace with intermittent stirring for 0.5 min. The molten glass was cast onto a carbon plate and annealed at 420^{o}C for 2h to release the internal stresses. Samples of 2 ± 0.01 mm thickness were prepared by cutting, grinding and polishing for optical measurements.

The UV-Vis absorption spectra in the range of 200-1100 nm were recorded using a double beam UV-visible spectrophotometer (Lambda 20, Perkin-Elmer) at an error of

±0.1 nm. The TEM, SAED and HRTEM images were taken using a FEI instrument (Tehnai-30, ST G^2) operating at an accelerating voltage of 300 kV. The instrument is also equipped with ultrahigh-resolution observation system.

Results and discussion

Bismuth glass dielectrics have great advantages over other types of glass dielectrics for its various technological applications as well as scientific study in the field of optoelectronics, photonics, various types of sensors etc (Peng et al. 2009; Ebendorff-Heidepriem et al. 2004; Ren et al. 2008). But these bismuth glass dielectrics have some drawbacks. These glasses show graying or blackening color when melted above 1000^{o}C. The intensity of graying or blackening enhance with the rise in melting temperature as well as Bi_2O_3 content. This intensification of color is due to auto-thermo reduction of Bi^{3+} ions to bismuth metal (Bi^o) during the process of melting. The reduction of Bi^{3+} ions to Bi^o occurs through the following thermal dissociation reaction (Zhang et al. 2008; Sanz et al. 2006)

$$2Bi_2O_3 \leftrightarrow 4Bi^o + 3O_2 \qquad E^o = 0.31V \qquad (1)$$

The metallic Bi^o is produced in a uncontrolled manner with the liberation of oxygen as shown in the above equilibrium reaction. This formation of metallic bismuth could be controlled by the oxidation process. Therefore, when the strong oxidizing agent, such as $K_2S_2O_8$, is added in the glass composition, it increases the oxygen partial pressure.

Thermal dissociation of $K_2S_2O_8$ during melting process at high temperature is as follow (Mellor 1947)

$$K_2S_2O_8 \leftrightarrow K_2O + 2SO_3\uparrow + \tfrac{1}{2} O_2\uparrow \qquad E^o = 2.01V \qquad (2)$$

$$2SO_3 \leftrightarrow 2SO_2\uparrow + O_2\uparrow \qquad (3)$$

Therefore, the reaction of the equation (1) proceeds in the reverse direction due to reactions of the equations. (2) and (3). By comparing the standard reduction potentials**,** it is clear that the standard potential of $S_2O_8^{2-}/SO_4^{2-}$ is much higher (2.01 *V*) than that of Bi^{3+}/Bi^o (0.31 *V*) species (Vanýsek 1994). Therefore, it easily favors the backward reactions of the equation (1) which results in controlled formation of Bi^o nanoparticles (NPs) and increases the transparency of the glasses. The UV-visible absorption spectra in figure 1 show a surface plasmon resonance (SPR) band at 460 nm in the presence of strong oxidizing agent ($K_2S_2O_8$) due to the existence of bismuth nanoparticles. Such prominent SPR band is not appeared in the bismuth glass which does not contained $K_2S_2O_8$ due to presence of comparably massive amount of bigger size bismuth particles. In this study, the intention of using strong oxidizing agent is to control the formation of Bi^0 NPs and therefore, the transparency of the bismuth glass dielectric enhances to a great extent.

The electron beam irradiation during the TEM experiment at an accelerating voltage of 300 kV performed on the bismuth glass dielectrics containing 0.5 wt % $K_2S_2O_8$ at various time intervals and the resultant images are shown in the figure 2. The

TEM images at the initial stage (0 min) of electron beam (EB) irradiation in figure 2 (a) clearly reveal the homogeneously dispersed and densely embedded very small Bi^o NPs and their size range 1-2 nm. This controlled size of bismuth NPs are achieved due to the addition of strong oxidizing agent $K_2S_2O_8$ in the bismuth glass. Its selected-area electron diffraction (SAED) pattern is shown in figure 3 (a) which has not revealed any distinct spots due to the very small particle size (1-2 nm). But, at 2 min of EB irradiation, the sample shows prominent Bi NPs growth with the size range 4-5 nm. Here, the overall shape of the sample is also changed to about oblate by contraction and densification. The TEM image observed at 4 min of EB irradiation show comparable bigger particle size (5-9 nm) and overall shape became spherical, which is demonstrated in the figure 2 (c). Its SAED depicts the clear patterns of <410> *hkl* plane of rhombohedral metallic Bi nanoparticles, which have been identified from the d-spacing (JCPDS File Card No.: 05-0519). When the time of irradiation increases to 8 min the particle size increases to 8-11 nm as shown in figure 2 (d). Its electron diffraction pattern revealed the <104> and <101> *hkl* crystalline planes of rhombohedral Bi NPs (JCPDS File Card No.: 05-0519) which is shown in figure 3 (c). Some SAED patterns in the images are not well defined; hence these could not be identified. A representative high resolution transmission electron microscopy (HRTEM) image of 8 min of EB irradiation is shown in figure 3 (d) which shows the characteristic lattice fringes measured to be 0.234 nm corresponds to the <104> *hkl* planes of the rhombohedral bismuth [space group: $R\bar{3}m$(166)] with lattice constants a = 4.546 Å and c = 11.86Å (JCPDS File Card No.: 05-0519).

The TEM images for the sample following electron beam irradiation for 8 min reveals the density of Bi particles in the sample is higher than that in the samples with

shorter time of irradiation. The average particle size increases with the EB irradiation time and this phenomenon is shown in the figure 4 which reveals that the average particle size gradually increases up to 11 nm for an EB irradiation time of 8 nm. This result suggests the possible control of the size and the density of the Bi nanoparticles in bismuth glass by varying the irradiation time of electron beam. The SAED patterns clearly show diffraction spots corresponding to the Bi crystal randomly distributed in plane with increase in irradiation time. Kim et al. 2007 and Sepulveda-Guzman et al. 2007 have also found the similar findings for the formation of bismuth nanoparticles trough electron beam irradiation in TEM. Sepulveda-Guzman et al. 2007 demonstrated that once the smallest bismuth nanoparticles is formed, then these nanoparticles acted as seeds and grew into crystals. Some of the nanoparticles were competent to grow into large crystals by the Ostwald ripening process. In the initial stage of electron beam irradiation, the bismuth nanoparticles were too small and exhibited a rapid movement. When the particle size increases, the movement became slow down and became more stable under the electron beam observation. In this study, we have also observed the similar phenomena which facilitated to observe the HRTEM image for the bigger particle (EB irradiated for 8 min) than that of smaller size due to its comparable more stability. Here, the crystal structure of the particles could not clearly define when they were very small. But, with the assistance of the TEM electron beam irradiation, the smaller particles as shown in figure 2 (a) seem to merge with each other to make bigger particles, showing a smoother surface (figure 2 (b-d)). These results show that Bi NPs randomly dispersed and gathered in the glass matrix to nucleate assisted by the electron beam irradiation energy. Bismuth

has a low melting temperature (271^0C) and this contributes to such energy induced structural change phenomena during in situ TEM observations.

Latheam at el. 2008 have demonstrated the TEM induced changes to the morphology of amorphous Fe, Co, and Ni metal oxides nanoparticles. In this study they observed that the nanoparticles are transforming from initial solid spheres to core, void or shell structures and finally to hollow nanoparticles. Oshima et al. 1997 have found very interesting structural anomaly of bismuth particle at a critical size of 8.4 nm. The bismuth particles smaller than the 8.4 nm revealed the rhombic structure, whereas the particle size increases above the critical size it transformed to cubic structure. But in our study, we have found only rhombohedral structure of bismuth for the various particle sizes.

Some previous studies done by various researchers in this field have revealed that the growth and morphology of the bismuth NPs carried out through electron beam irradiation depend on various parameters such as EB irradiation dose and time duration, temperature and particle size. Derrouiche et al. 2010 have demonstrated how morphology of bismuth nanoparticles is changes with respect to electron beam irradiation. The increase in the size of the particles arises due to coalesce of two or more particles. If r_1, r_2, r_3, ……., r_i are the radii of particle p_1, p_2, p_3, ……, p_i, then under the electron beam, p_1 moves across the surface and join particle p_2, it gives unique particle of radius R which can be expressed as:

$$R = [\Sigma\, r_i^3]^{1/3} \qquad (4)$$

The process of formation, growth and then coalesce of bismuth nanoparticles is an irreversible process.

Meldrum et al. 2000 have show how the effects of ion irradiation can be used to good advantage in the formation of novel nanocrystal microstructures and nanocrystal-host structural relationships and its nanolithography application. Their results were somewhat amazing that the amorphous material crystallized to form a nanometer-scale polycrystalline assemblage of $ScPO_4$ within a matter of seconds depending on the beam-current density. This crystallization process could be controlled by focusing the electron beam and moving the focal point with the beam shift controls through TEM. In this method, letters and patterns of nanocrystals could be drawn easily in the amorphous host matrix. Therefore, our study based on electron beam irradiation on the bismuth glass dielectric which is technologically very important material could also be useful for the nanolithography as well as nanopaterning for integrated nanooptics applications due to the rapid formation (within the a minute) of bismuth nanocrystal in the bismuth glass dielectric it self.

Conclusion

This study revealed a simple but very effective methodology to control the synthesis of the Bi nanoparticles in bismuth glass dielectrics using electron beam irradiation in TEM. The bismuth nanoparticles size increases with the electron beam irradiation time. This type of electron beam irradiation induced change in morphology is attributed to the low melting temperature of bismuth metal. The well-defined Bi nanoparticles show the rhombohedral structure which is common in bulk bismuth. This work is very important

for nanolithography and nanopaterning in optoelectronics applications due to rapid formation of bismuth nanocrystal in bismuth glass dielectrics.

Acknowledgements SPS express his sincere gratitude for the financial support of the Council of Scientific and Industrial Research (CSIR), New Delhi in the form of CSIR-SRF under sanction number 31/15(78)/2010-EMR-I. The authors thank Director of the institute for his kind permission to publish this paper. They also thankfully acknowledge the Electron Microscope Division of this institute for recording the TEM, HRTEM and SAED images.

References

Balan L, Schneider R, Billaud D, Fort Y, Ghanbaja J (2004) A new synthesis of ultrafine nanometre-sized bismuth particles. Nanotechnology **15:** 940-944.

Carotenuto G, Hison CL, Capezzuto F, Palomba M, Perlo P, Conte P (2009) Synthesis and thermoelectric characterisation of bismuth Nanoparticles. J Nanopart Res 11:1729–1738.

Derrouiche S, Loebick CZ , Pfefferle L (2010) Optimization of Routes for the Synthesis of Bismuth Nanotubes: Implications for Nanostructure Form and Selectivity. J Phys Chem C 114: 3431-3440.

Ebendorff-Heidepriem H, Petropoulos P, Asimakis S, Finazzi V, Moore RC, Frampton K, Koizumi F, Richardson DJ, Monro TM (2004) Bismuth glass holey fibers with high nonlinearity. Opt Express 12: 5082-5087.

Gao Y, Niu H, Zeng C, Chen Q (2003) Preparation and characterization of single-crystalline bismuth nanowires by a low-temperature solvothermal process. Chem Phys Lett 367: 141-144.

Gekhtman D, Zhang ZB, Adderton D, Dresselhaus MS and Dresselhaus G (1999) Electrostatic Force Spectroscopy and Imaging of Bi Wires: Spatially Resolved Quantum Confinement. Phys Rev Lett 82: 3887-3890.

Grass RN, Stark WJ (2006) Flame spray synthesis under a non-oxidizing atmosphere: Preparation of metallic bismuth nanoparticles and nanocrystalline bulk bismuth metal. J Nanopart Res 8: 729–736.

Grzelczak M, Pe´rez-Juste J, Mulvaney P, Liz-Marza´n LM (2008) Shape control in gold nanoparticle synthesis. Chem Soc Rev 37: 1783-1791.

Jana N R, Gearheart L and Murphy C J 2001 Seeding Growth for Size Control of 5-40 nm Diameter Gold Nanoparticles. Langmuir 17: 6782-6786.

Kim J-U, Cha S-H, Shin K, Jho JY, Lee J-C (2005) Synthesis of Gold Nanoparticles from Gold(I)-Alkanethiolate Complexes with Supramolecular Structures through Electron Beam Irradiation in TEM. J Am Chem Soc 127: 9962-9963.

Kim SH, Choi Y-S, Kang K, Yang SI (2007) Controlled growth of bismuth nanoparticles by shiv beam irradiation in TEM. J Alloy Compd 427: 330-332.

Latham AH, Williams ME (2008) Transmission Electron Microscope-Induced Structural Evolution in Amorphous Fe, Co, and Ni Oxide Nanoparticles. Langmuir 24: 14195-14202.

Meldrum A, Boatner LA, White CW, Ewing RC (2000) Ion irradiation effects in nonmetals: formation of nanocrystals and novel microstructures. Mat Res Innovat 3: 190-204.

Mellor JW (1947) Comprehensive Treatise on Inorganic and Theoretical Chemistry. Vol. IX Longmans, London

Oshima Y, Takayanagi K, Hirayama H (1997) Structural anomaly of fine bismuth particles observed by ultra high-vacuum TEM. Z Phys D 40: 534-538.

Peng M, Wondraczek L (2009) Bismuth-doped oxide glasses as potential solar spectral converters and concentrators. J Mater Chem 19: 627-630.

Ren J, Dong G, Xu S, Bao R, Qiu J (2008) Inhomogeneous Broadening, Luminescence Origin and Optical Amplification in Bismuth-Doped Glass. J Phys Chem A 112: 3036-3039.

Sanz O, Haro-Poniatowski E, Gonzalo J, Navarro JMF (2006) Influence of the melting conditions of heavy metal oxide glasses containing bismuth oxide on their optical absorption. J Non-Cryst Solids 352: 761-768.

Sepulveda-Guzman S, Elizondo-Villarreal N, Ferrer D, Torres-Castro A, Gao X, Zhou JP, Jose-Yacaman M (2007) *In situ* formation of bismuth nanoparticles through electron-beam irradiation in a transmission electron microscope. Nanotechnology. 18: 335604 (1-6).

Vanýsek P (1994) Electrochemical Series, in CRC Hand Book of Chemistry and Physics. Edited by Lide DR, CRC Press, London

Wang D, Ma X, Wang Y, Wang L, Wang Z, Zheng W, He X, Li J, Peng Q, Li Y (2010) Shape Control of CoO and $LiCoO_2$ Nanocrystals. Nano Res 3: 1–7.

Wang F, Tang R, Yu H, Gibbons PC, Buhro WE (2008) Size- and Shape-Controlled Synthesis of Bismuth Nanoparticles. Chem Mater 20: 3656-3662.

Wang YW, Hong BH, Kim KS (2005) Size Control of Semimetal Bismuth Nanoparticles and the UV-Visible and IR Absorption Spectra. J. Phys. Chem. B 109: 7067-7072.

Zhang Y, Yang Y, Zheng J, Hua W, Chen G (2008) Effects of Oxidizing Additives on Optical Properties of Bi_2O_3–B_2O_3–SiO_2 Glasses. J Am Ceram Soc 91: 3410-3412.

Zhang ZB, Gekhman D, Dresselhaus MS, Ying JY (1999) Processing and Characterization of Single-Crystalline Ultrafine Bismuth Nanowires. *Chem. Mater.* 11: 1659-1665.

Figure Captions

Fig. 1 Absorption spectra of (a) without and (b) with 0.5 wt % $K_2S_2O_8$ in the glasses

Fig. 2 TEM images of the bismuth nanoparticles in bismuth glass at (a) 0, (b) 2, (c) 4 and (d) 8 min time interval of electron beam irradiation

Fig. 3 Selected area electron diffraction (SAED) images of the bismuth nanoparticles in bismuth glass during various time interval of electron beam irradiation at (a) 0, (b) 4 and (c) 8 min, and (d) high resolution transmission electron microscopy (HRTEM) at 8 minute

Fig. 4 Average bismuth nanoparticle size (nm) as a function of time (min) of electron beam irradiation

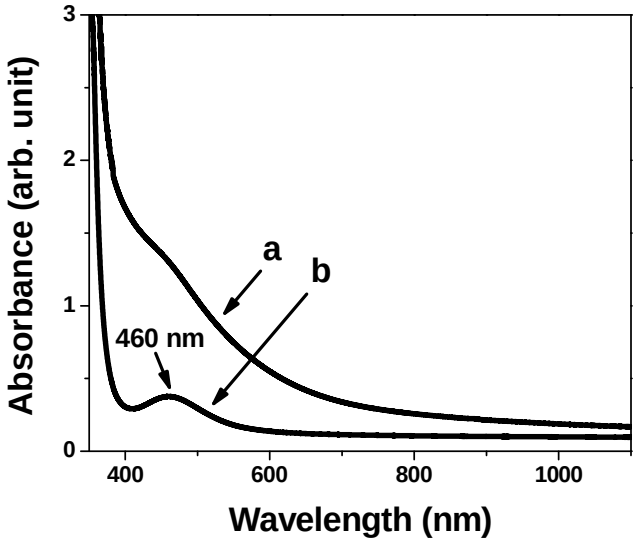

Fig. 1 Absorption spectra of (a) without and (b) with 0.5 wt % $K_2S_2O_8$ in the glasses

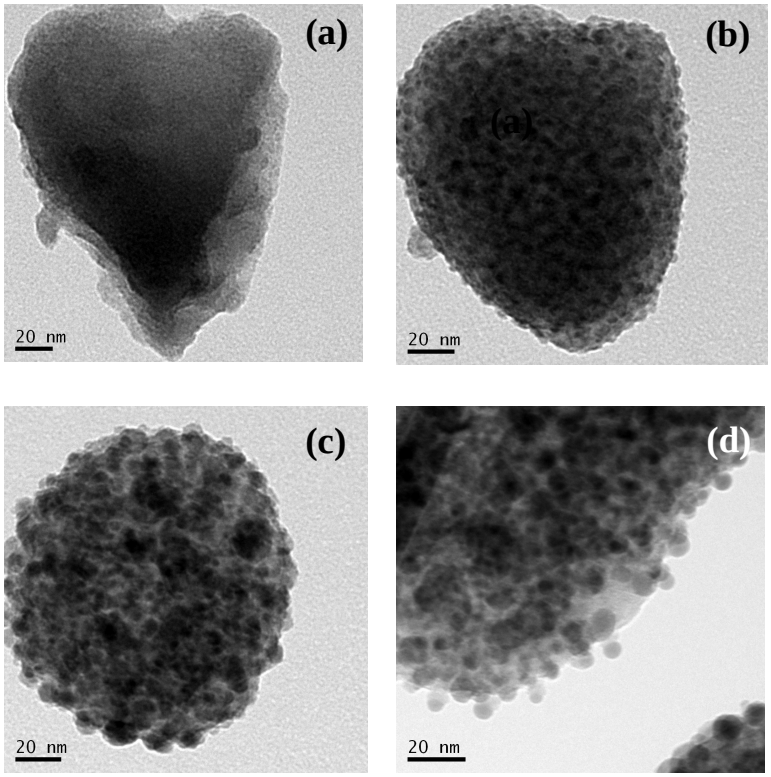

Fig. 2 TEM images of the bismuth nanoparticles in bismuth glass at (a) 0, (b) 2, (c) 4 and (d) 8 min time interval of electron beam irradiation

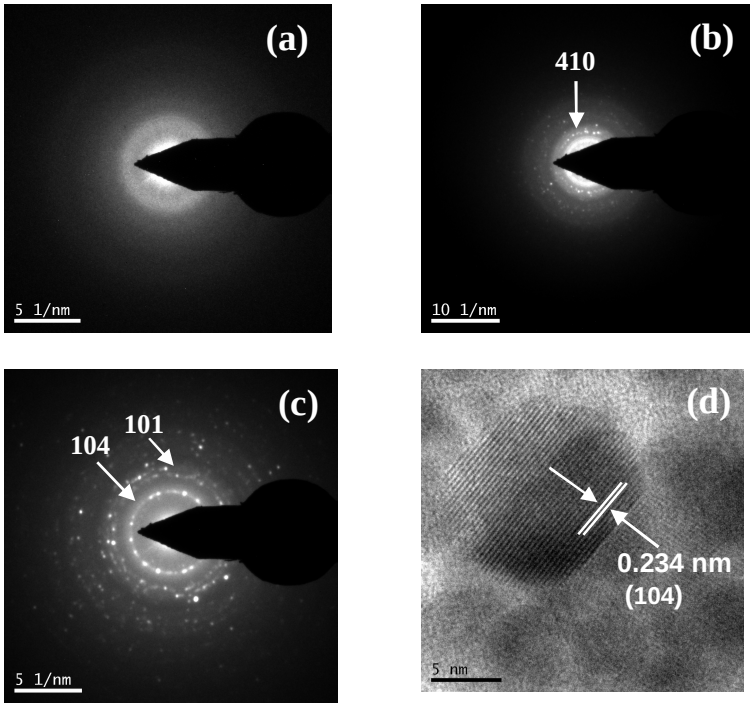

Fig. 3 Selected area electron diffraction (SAED) images of the bismuth nanoparticles in bismuth glass during various time interval of electron beam irradiation at (a) 0, (b) 4 and (c) 8 min, and (d) high resolution transmission electron microscopy (HRTEM) at 8 minute

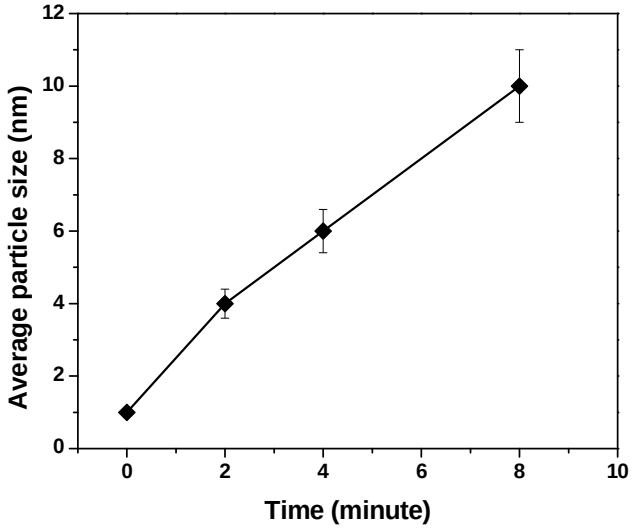

Fig. 4 Average bismuth nanoparticle size (nm) as a function of time (min) of electron beam irradiation